



Wastewater treatment and electricity generation via microbial fuel cell using ZnO supported on activated carbon cathode electrocatalyst



CrossMark

Doaa Khodary^a, Fatma I. Elzamik^a, Howaida M. Abdel basit^a, G. M. Moustafa^a,
and K. M. El-Khatib^{b,*}

^a Microbiology Department, Faculty of Agriculture, Zagazig University, Zagazig City, El-Sharqia, Egypt, 44511.

^b Chemical Engineering & Pilot Plant Department, Engineering and Renewable Energy Research Institute, National Research Centre, 33 El-Buhouth St., Dokki, Cairo 12311, Egypt

Abstract

Microbial fuel cells are bio-electrochemical devices that use extracellular electron transfer (EET) to promote anaerobic biodegradation of biomass to generate electricity and clean wastewater. In this study, Zinc oxide supported on activated carbon (ZnO/AC) is investigated as a cathode electrocatalyst and compared with a benchmark Pt/C electrocatalyst. Electrochemical measurements of the ZnO/AC electrocatalyst were performed utilizing a rotating disc electrode (RDE) and linear sweep voltammetry (LSV) in a phosphate buffer solution (pH 7). Furthermore, its long-term performance in a single chamber MFC application is assessed by evaluating organic matter elimination and polarisation behaviour. Finally, scanning electron microscopy is used to check the surface morphology of the bio anode. It could be observed that ZnO/AC shows high selectivity towards the oxidation reduction reaction (ORR). In addition, it displays the highest achievable power density generation value of 90.177 mW m^{-3} at cell current density of $300.295 \text{ mA m}^{-3}$, where the Pt/C cathode generates a high power density of $128.054 \text{ mW m}^{-3}$ at a cell current density of $357.846 \text{ mA m}^{-3}$. Our results indicate that the ZnO/AC cathode is improved electrocatalytic performance toward ORR in a pH-neutral solution, making it a viable substitute for pricey Pt-based catalysis.

Keywords: Microbial fuel cell; ZnO/AC; Linear Sweep Voltammetry; wastewater treatment, electricity generation

Introduction

Energy insecurity and climate change, which are driven by the depletion of fossil fuels and global warming, respectively, must be urgently addressed if the modern world is to avoid further catastrophes. In recent years an international energy crisis resulted from the acceleration of fossil fuels consumption. A viable solution to the present global warming problem is renewable energy resources. However, efforts have been made to create alternative power-producing mechanisms. It is also desired to generate electricity using clean energy resources with really no net carbon dioxide emissions. [1, 2].

Microbial Fuel Cell (MFC) is a bioelectrochemical device that transforms chemical energy from biodegradable wastewater into electrical energy using electrochemically active microorganisms (EAMs) as biocatalysts [3, 4]. MFCs are frequently regarded as a perfect source of energy

due to their low-maintenance operation, minimal emissions, and most crucially, an infinitely renewable source of reactants [5, 6]. The adaption of EAM on the anodic surface and the resulting biofilm are the key steps in MFC current production [7].

The MFC generally has two chambers, among which is called an anodic (anaerobic) chamber and the other is called a cathodic (aerobic) chamber, where the reduction occurs [8]. In the anode chamber, microorganisms oxidize the organic substrate to release protons (H^+) and electrons. An external circuit that generates electricity transfers electrons to the cathode chamber. Water is formed when H^+ ions pass through the membrane and combine with oxygen in the cathode chamber. Wastewater serves as a fuel for microbial activities in the anodic chamber. The amount of organic matter (substrate), pH, overall dissolved solids, and other factors all influence the kinetics of a biochemical process in an anodic

*Corresponding author e-mail: kamelced@hotmail.com; (K. M. El-Khatib).

Receive Date: 11 March 2023, Revise Date: 29 April 2023, Accept Date: 03 May 2023

DOI: 10.21608/EJCHEM.2023.199316.7716

©2023 National Information and Documentation Center (NIDOC)

chamber. Experimentation is frequently achieved by optimizing the flow rate of effluents based on the energy of bacterial growth [9].

Physiological (external resistance, pH, flow rate, and temperature), physical (cell configuration, electrode materials, and membrane), and biological (substrate type, microorganism, and electron transfer methods in microorganisms) characteristics greatly impact power generation [10]. The oxidation reaction of the reactant molecules, the electron transport for both bacteria and the anode, the oxidation reduction reaction (ORR) mechanisms on the cathode, and ohmic/mass transport losses are a few parameters that influence MFC efficiency [11]. Among them, the ORR pathway here on the cathode is a key element to significantly determine the performance of the MFC in general. Platinum-based nanoparticles have been used extensively as cathodic materials for MFC applications because of their high electrocatalytic activity toward ORR, and their implementations have just been severely restricted because of their high prices and unsuitable durability beneath MFC conditions [12]. Materials derived from non-noble metal precursors have been widely used as active components in ORR electrocatalyst is due to their high natural abundance, low cost, and obvious electrocatalytic activity. [13].

The well-known electrode materials for MFCs are carbon-supported materials, like carbon fabric [14], carbon paper [15], carbon felt [16], carbon fiber [17], and graphite particles [18].

Transition metal oxides (TMOs) are considered replacement candidates instead of Platinum, due to their superior physical and chemical properties, wide structural variation, excellent catalytic activity, non-toxicity, and eco-friendliness [19]. ZnO has sparked considerable interest in the research community and industrial applications [20]. Adsorbent techniques could be used for reducing Cu^{+2} , Zn^{+2} , Ni^{+2} and other ions from wastewater treatment as steel pipelines [21] or Montmorillonitic clay [22]. Whereas, these previously ions could be used as active cathodic electrocatalysts for treatment of organic substrate in MFC. According to its poor electro conductivity, which may hinder very much its application as an electrode substance in the oxygen reduction reaction (ORR) action, thus it is requisite to integrate ZnO with activated carbon layers.

To date, there are insufficient studies that have investigated the use of Zn-based as efficient ORR electrocatalyst. Mathew and Thomas [23] used PANI-Cu/ZnO nanoparticles for double chambered MFC application generating a power density of 45.120 mWm^{-2} . In another research, Khajeh et al.

[24] evaluated a dual-chamber MFC that use CuO/ZnO-modified graphite plates and reported a power density of 51.84 mWm^{-2} under visible light irradiation. Furthermore, Yang et al. [25] studied the nanocomposites (GO-Zn/Co) made of graphene oxide-loaded cobalt and zinc oxide nanoparticles followed by pyrolysis at controlled temperatures. This method demonstrated that the GO-Zn/Co (1:1) catalyst displayed the highest ORR performance, with a high half-wave potential of $+0.81 \text{ V}$ compared to a maximum power density of (773 mW m^{-2}) for Pt/C. Additionally, Yu et al. [26] investigated the effectiveness of ZnO nanoparticles (NPs) with reduced graphene oxide (rGO) as an oxygen-reduction electrocatalyst. The hierarchical ZnO/rGO hybrid nanomaterial demonstrated excellent electrocatalytic activity for ORR due to its high cathodic current density ($9.21 \cdot 10^{-5} \text{ mAcm}^{-2}$), low H_2O_2 yield (less than 3%), positive onset potential (-0.2 V), and high electron transfer numbers. On another hand, Yi et al. [27] demonstrated that Zn-doped perovskite oxide $\text{CaFe}_{0.7}\text{Zn}_{0.3}\text{O}_3$ nanoparticles for a dual chamber and investigated the high output voltage was 0.428 V which is greater than Pt/C (0.378 V) and has a power density of 892.10 mW m^{-3} .

Wang et al. [28] discovered that Zn-Ni-Co spinel oxides outperformed NiCo_2O_4 in terms of ORR because the Zn element effectively optimized the pore structure of the catalyst and improved the exposure density of the active site. Camacho et al. [29] developed a series of oxide-carbon composites using various oxides (TiO_2 , SnO_2 , ZnO) and selected platinum deposition on to oxide sites to achieve Pt/ TiO_2 -C, Pt/ SnO_2 -C, and Pt/ ZnO -C. They discovered that Pt/oxide-carbon compounds had better ORR activity than Pt/C catalysts. Moreover, Mahalingam et al. [30] studied the feasibility of reduced graphene oxide-copper sulfide-zinc sulphide nano composite cathode electrocatalyst in SCMFCs and obtained a high power density of ($1692 \pm 15 \text{ mWm}^{-2}$) and OCP ($761 \pm 9 \text{ mV}$). In addition, Bahamonde et al. [31] used Cel-PDA/ TiO_2 :ZnO nanoparticles for a single chamber and yield a power density of 63 mWm^{-2} . Furthermore, Abdullah Mirzaie et al. [32] Investigated Pt/ZnO/SWCNT 30 wt. % electrocatalyst showing great catalytic activity for the ORR and obtained a current density of $70.885 \text{ mA cm}^{-2}$ and having greater catalytic activity than carbon used in Pt/C.

The purpose of this research was to employ ZnO/AC based MFC through aerobic activated sludge as a substrate to optimize the efficiency of ORR and electroactive microbial activities while also removing organic matter via wastewater treatment and electricity production. In this work, the application of ZnO/AC as cathode electrocatalyst to improve the

MFC performance was explored. The electrochemical characteristics and electron-transfer number of ZnO/AC were investigated using linear sweep voltammetry (LSV) in neutral media (PBS, pH=7). The performance of the ZnO/AC was then compared to that of a commercial Pt/C in air-cathode MFCs by measuring power density and polarisation behaviour. Finally, scanning electron microscopy (SEM) was used to examine the physical properties of the generated biofilm.

Materials and methods

Materials

Zinc oxide (ZnO) and 5 wt. % Nafion solutions are purchased from Sigma-Aldrich (USA). 30% Pt/C E-tek is supplied from Fuel Cell Store (TX, USA). All materials and supplies were of reagent grade purity and were not further purified. All aqueous solutions are made using double-distilled fresh water.

Preparation of ZnO /AC electrocatalyst

The as-received Carbon Vulcan XC-72R is chemically treated and cleansed in an ultrasonic bath with 8.0 M HNO₃ and 8.0 M H₂SO₄ (1:1, v:v) for 4 hours. After that, the product is filtered and washed many times with double-distilled water before drying for 6 hours at 80 °C [16]. The activated carbon support material for the synthesis of ZnO/AC (30 wt. %) is treated with acid.

Electrochemical evaluation of electrocatalysts

A VoltaLab 6 electrochemical workstation and a rotating disc electrode (RDE; CTV 101 speed control unit) linked to a personal computer are used for the electrochemical measurements. An Ag/AgCl electrode and platinum (Pt) wire were employed as reference and counter electrodes in a traditional three-electrode electrochemical cell arrangement. The working electrodes are ZnO and AC electrocatalysts are coated as an ultra-thin layer on a glassy carbon (GC) disc electrode that is part of the RDE. Before catalyst deposition, the GC electrode (which has a geometrical surface area of 0.196 cm²) is mechanically polished to create a mirror-like surface using 0.05 m alumina slurry and a soft cloth. It was then cleaned with deionized water and acetone. The catalyst ink is prepared by combining 2.5 mg of the electrocatalysts with 15 L of a 5% Nafion solution and 0.5 ml of isopropanol. After sonication for 15 minutes, 5 µm of the ink is drop-cast onto the GC electrode.

The electron transfer numbers (n) involved in the ORR process are determined by analysing the kinetic parameters using the Koutechy-Levich (K-L) equation developed from RDE investigations [33] as follows:

$$\frac{1}{I_d} = \frac{1}{I_k} + \frac{1}{0.62nFAD^{2/3}cv^{-1}\omega^{1/2}} \quad (\text{Eq. 1})$$

Where I_d is the current density; I_k is the electrode potential; ω is the angular momentum (rads⁻¹s^{1/2}); n is the average number of electrons; F is Faraday's constant (96,485 C mol⁻¹); C and D are the concentration of dissolved oxygen in 50 mM PBS (1.117 × 10⁻⁶ mol mL⁻¹) and the dissolved oxygen diffusion coefficient (1.9 × 10⁻⁵ cm²s⁻¹), respectively; ν is the kinetic viscosity of the electrolyte (0.01073 cm²s⁻¹); and A is the geometric area of the electrode (0.196 cm²) [34].

ZnO/AC preparation for MFC cathode construction

The cathode electrode is made according to a procedure mentioned elsewhere [16]. The catalyst is kept on the water-facing side of a cathode at a mass loading of 0.3 mg cm². Before coating, catalyst slurry is made by combining ZnO/AC composites with a 5% Nafion solution. The mixture is ultrasonicated for 30 minutes at 60 °C and uniformly dispersed onto the carbon cloth surface electrode. Before MFC experiments, the electrode was dried at room temperature for 24 hours. In comparison, 30 wt.% of a Pt/C catalyst is used as cathode electrocatalyst using the same procedure as previously described.

Microbial fuel cell construction

Air-cathode single-chamber MFCs (4.6 cm in diameter, 6 cm long, total working capacity is 100 mL) are used for all MFC testing, as shown in Fig (1). Gas diffusion carbon cloth electrodes are employed as cathode electrodes, with a catalyst loading of 0.30 mg cm⁻², and three-dimensional carbon felt electrodes served as anodes attached to the top of an externally linked anode port.



Figure 1: Air cathode single chamber MFC.

Analysis and performance of MFCs

MFCs were injected with aerobic-activated sludge from a nearby municipal wastewater treatment facility (Minia El-Kamh, Egypt) and fed-batch operated for 60 days to allow biofilm to form on the anode surfaces. MFCs are fed with synthetic wastewater containing 1.0 g L⁻¹ of sodium acetate as a source of organic substrate in 50 mM phosphate buffer solution (PBS) supplemented with a 12.5 mL

mineral solution. The buffer solution contained: NaHCO_3 : 2.5 g/L, NH_4Cl : 0.2 g/L, KH_2PO_4 : 13.6 g/L, KCl : 0.33 g/L, NaCl : 0.3 g/L, K_2HPO_4 : 17.4 g/L, $\text{CaCl}_2 \cdot 2\text{H}_2\text{O}$: 0.15 g/L, MgCl_2 : 3.15 g/L, and yeast extract: 1 g/L. To obtain average results, all MFC experiments were performed in triplicate. MFCs were run in fed-batch mode and monitored using a data acquisition system (USB 6000 12 - BIT 10 KS/S Multifunction I/O AS WELL AS NI - DAQMX Software) linked to a personal computer. The polarization and power curves are created by measuring the steady-state voltage across external resistances ranging from 240Ω to $470\text{k}\Omega$. COD concentrations are determined using APHA standard procedures for water and wastewater analysis APHA 2005 [35]. COD removal efficiency (COD R%) is used to compute organic concentrations, which was calculated using the following equation [36]:

$$\text{COD R\%} = \frac{\text{COD}_{\text{initial}} - \text{COD}_{\text{final}}}{\text{COD}_{\text{initial}}} \times 100 \quad (\text{Eq. 2})$$

Where $\text{COD}_{\text{initial}}$ is the COD concentration in the influent (mg COD/L) and $\text{COD}_{\text{final}}$ is the COD concentration in the final outflow at the conclusion of MFC batch cycles (mg COD/L).

The Coulombic efficiency (C_E) is determined via integrating the current measured with respect to the theoretical current based on consumed COD as follows:

$$C_E(\%) = \frac{C_P}{C_T} \times 100 \quad (\text{Eq. 3})$$

Where C_T is the theoretical coulombs and was estimated using the following equation: $C_T = (F \times N \times W \times V) / M$, where F is Faraday's constant ($96,485 \text{ C mol}^{-1}$), N is the number of electron (8 mol mol^{-1}), W is the daily COD load removed (g), M is the molecular weight of acetate (59 gmol^{-1}), and V is the medium volume (100 mL) [28]. C_P is the Coulombs equivalent to the actual current produced during one batch cycle.

Scanning electron microscopy analysis of biofilms

At the end of batch studies, SEM analysis using (JEOL JAX-840A, Japan) is used to characterize anodic biofilm formation on bio anode electrode surfaces. The anode is fixed for 4 hrs in 2.5% (w/v) glutaraldehyde. Then the samples are washed three times in double distilled water and dehydrated in arising ethanol gradient steps (30% – 100% with 10 min for each step). Finally, all samples are sputtered with gold and imaged using SEM at 20 kV [37].

Results and Discussion

Electrochemical measurements using a rotating disk electrode.

The polarization curve of Pt/C and ZnO/AC electrodes in O_2 -saturated PBS at scan rates of 10 mV s^{-1} and rotation speeds of 1600 rpm is displayed in Fig. (2). It could be observed that the ZnO/AC reveals a lower positive onset potential (E_{onset} at 86 mV) as compared with Pt/C electrocatalyst (E_{onset} , 400mV). Furthermore, it exhibits a diffusion-limiting current density value of 3.19 mA cm^{-2} at 600 mV (vs. SHE) which is lower than Pt/C (5.09 mA cm^{-2}) with the identical potential value.

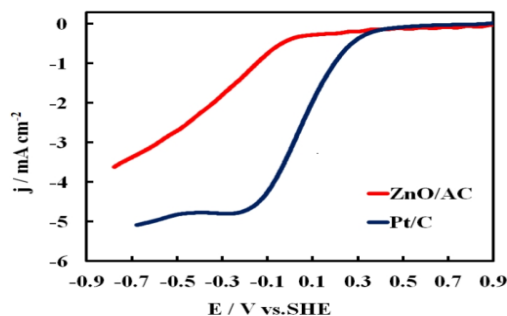
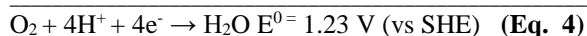


Figure 2: LSV curves of Pt/C and ZnO/AC cathodes at scan rate of 10 mV s^{-1} and rotation rate of 1200 rpm in O_2 -saturated 50 mM PBS at 25°C

To investigate the diffusion zone of current density for ZnO/AC, the polarization curve of LSV is conducted at distinct rotation speeds ranging from 400 to 2400 rpm in O_2 -saturated 50 mM PBS at a scanning rate of 10 mV s^{-1} as shown in Fig.3(a). The reduction current density improved by raising the rotating speed from 400 to 2400 and reducing the potential scan rate to a more passive side, as a consequence of increasing the quantity of diffused oxygen on the electrode surface indicating a controlled kinetics process [38].

In addition, the reduction current density improved from -1.45 to -3.75 mA cm^{-2} while increasing in rotation speed from 400 to 2,400 rpm and decreasing the potential scan to much more negative values. As shown in Fig. 3(b), the polarisation curve data is used to plot K-L relationships, where the inverse current density (j^{-1}) is directly proportional to the inverse root square of the rotation speed ($1/2$) over different potential ranges (i.e., 200 to - 400 mV vs. SHE). The K–L graphs for both electrocatalysts are parallel and linear, indicating enhanced ORR electrocatalytic activity (kinetically more facile). The calculated number of electrons involved in ORR (n) is derived from the slopes of the K-L plot as follows: 3.86, 3.5, and 3.3 at -200 , 300, and 400 mV, respectively. It is suggesting that electrocatalytic ORR is catalysed via a direct, one-step, four-electron transfer pathway (as shown in Eq. 4).



As a result of the combined influence of ZnO and AC placed onto carbon fabric, catalytic activity toward ORR was detected. Additionally, the large catalytic surface area of ZnO/AC particles facilitated rapid deposition rates of the catalyst onto the surface of activated carbon, as did the material's high porosity. Our findings show that cheaper Pt-free metal oxides may be used as electrocatalysts in MFCs without considerably reducing performance. It was concluded that ZnO/AC significantly improved redox reaction performance and demonstrated electrochemical behaviour toward ORR comparable to Pt in neutral electrolytes, and it may be used for a wide range of MFC applications because of its availability, low cost, the presence of oxidation states, and its high electrical conductivity.

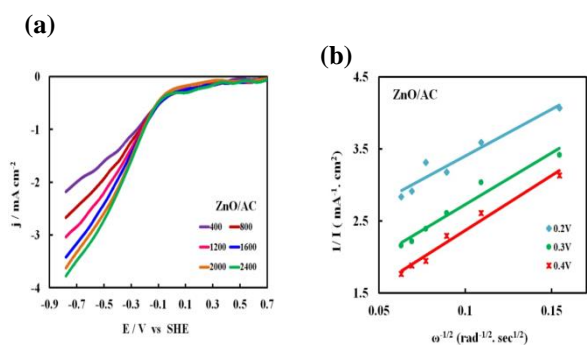


Figure 3: a) ORR polarization curve of ZnO/AC electrocatalyst at different rotation rates. b) The corresponding Koutecky–Levich plot potential from 0.2 to 0.4 V vs. SHE.

Microbial fuel cell performance

Acetate was used as an electron donor in MFCs under open circuit voltage (OCV), and the rates of electrochemical and biochemical response as well as the long-term stability of the ZnO/AC are estimated and compared to a Pt/C-based MFC Fig.4(a-b). Substance oxidation and a rise in OCV are caused by improvements in anodic metabolic activity in subsequent cycles. MFCs showed a consistent OCV of 598 mV for the Pt/C-based MFC and 562 mV for the ZnO/AC-based MFC after operating for 88 days. Both MFC's closed-circuit cell potentials are assessed across a 10 kΩ external resistance. Fig.4(c-d) depicts the potential generation (V) curves throughout three cycles as a function of the time (hrs). The ZnO/AC-based MFC has a slightly lower maximum closed-circuit voltage output than the Pt/C-based MFC (300 and 358 mV, respectively). The ZnO/AC cathode generated a maximum PD of 90.177 mW m⁻³ at a cell current density of 300.295 mA m⁻³, whereas the Pt/C cathode generated a maximum PD of 128.054 mW m⁻³ at a cell current density of 357.846 mA m⁻³ (Fig. 5(a-

b)). ZnO/AC has a lower internal resistance (70Ω) than Pt/C (120Ω).

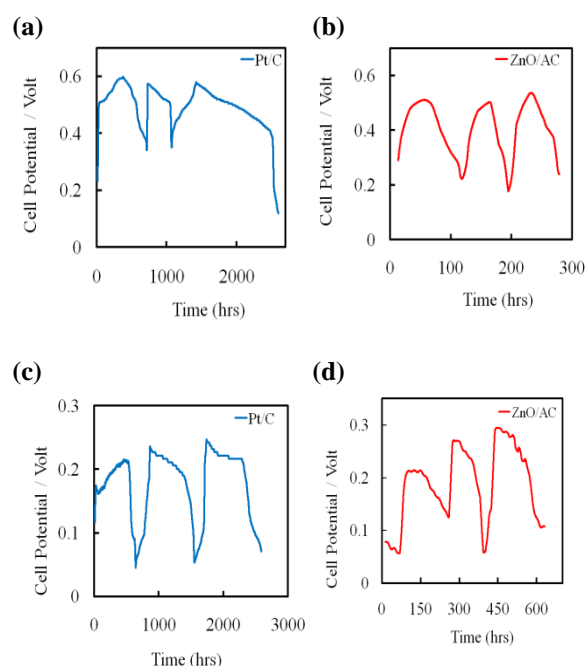


Figure 4 : OCV of a)Pt/C- and ,b) ZnO/AC based MFCs, CCV of c) Pt/C and d) ZnO/AC based MFCs at external resistance of 10 kΩ.

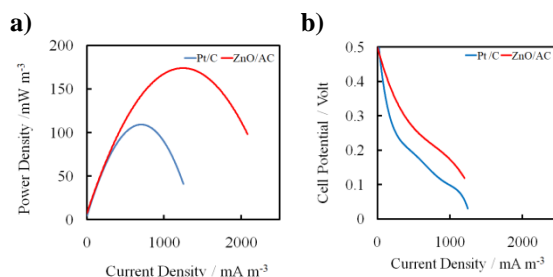


Figure 5: Power density a) and polarization curves b) for of Pt/C and ZnO/C based MFCs.

Organic matter removal

The COD removal percentage for the ZnO/AC-based MFC was 76.17 ± 17.18 % which was somewhat higher than the 55 ± 25.17 % for the Pt/C MFC. Moreover, ZnO/AC achieved coulombic efficiency (C_E) at 9.6 ± 2.41%, which was lower than Pt/C (C_E, 30 ± 17.34 %). These results showed that C_E was mostly driven by cathode fluctuations, but they may also be due to the perfect characteristics of the ZnO/AC electrocatalyst. The biofilm's production is based on the bacterial cell's active growth at a high COD removal value. More COD elimination is thought to be directly related to greater substrate usage and comparable higher performance with increasing power output [30].

Visualization of electroactive anodic biofilm

The surface morphologies of anodic biofilms on bare carbon-felt and carbon-felt electrode anodes are investigated using scanning electron microscopy

(SEM). The surface morphology of bare carbon felt, as shown in **Fig. (6)**, was extremely smooth, with many carbon fibers crossing one another to form a mesh-like structure. However, the surface and inner pores of the carbon-felt anodic biofilm entirely covered the anode. In addition, bacteria appeared from about 1.37 μm to 909 nm long. The proposed mechanism inside the MFC could be illustrated through two steps, first step; the anodic microbial diversities can degrade the acetate into protons and electrons. Second step; both electrons and protons are transferred into the cathode. The electrons are moved through an external circuit for generating the electricity. The protons are diffused to combine with oxygen to form water.

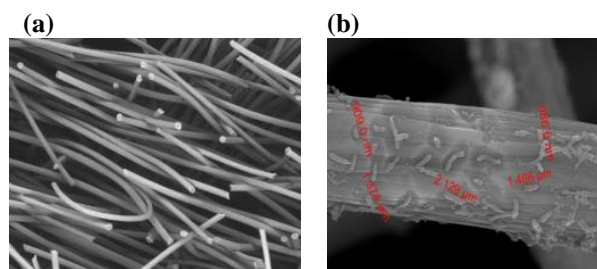


Figure (6): SEM images (a) for carbon felt- free anode before adding microbial community (b) morphological characters anodic biofilm.

The SEM study of the surface of anodic biofilms revealed rod-shaped bacterial cells suggestive of electroactive microorganisms, demonstrating that the capacity of the anodic electrodes to generate electricity was due to the presence of electroactive biofilms on their surface. In MFCs, non-precious ZnO/AC-based electrocatalysts displayed comparable catalytic activity and stability to Pt/C cathodes, according to a review of the relevant literature **Table (1)**. The high PD of MFCs demonstrates that ZnO-based electrocatalysts might be employed as cathode catalyts.

It was discovered that our electrocatalyst was more effective than that reported by **Mathew and Thomas [23]** these authors utilized polymer polyaniline (PANI) with ZnO nanoparticles PANI-ZnO and PANI-Cu/ ZnO, which yielded a PD of 7.044 mWm^{-2} and 45.120 mWm^{-2} , respectively. In another study, **Mahalingam et al.[30]** studied the feasibility of reduced graphene oxide-copper sulfide-zinc sulphide nanocomposite a cathode electrocatalyst in SCMFCs and obtained the high power density of (1692 \pm 15 mWm^{-2}) and OCP (761 \pm 9 mV). Moreover, **Yi et al.[27]** demonstrated that Zn-doped perovskite oxide $\text{CaFe}_{0.7}\text{Zn}_{0.3}\text{O}_3$ nanoparticles for a dual chamber and investigated the high output voltage was 0.428 V

which is higher than that of Pt/C(0.378 V) and a power density of 892.10 mW m^{-3} .

This variation in PD might be attributed to a variety of factors, including operating environment, MFC structure, anode kind, surface area, microbial community variations, and changes in electrocatalyst supporting substance and expected surface area.

Conclusion

The current study focuses on the application of ZnO/AC as a cathode electrocatalyst in MFCs application. Electrochemical measurements of ZnO/AC electrocatalysts were conducted using RDE and LSV in PBS (pH 7). The electrochemical study suggests that the ZnO/AC electrocatalyst has good selectivity and electrochemical stability towards the ORR that follows the four-electron pathway. The highest PD of ZnO/AC -based MFCs was 90.177 mW m^{-3} and the CE was 9.6 \pm 2.41%, which is comparable to Pt/C-dependent on MFCs (PD = 128.054 mW m^{-3} and CE = 30 \pm 17.34 %) under the same condition. The rod-shaped morphology of electroactive bacteria was shown by SEM examination of anodic biofilm, demonstrating that the produced electricity was caused by the electroactive biofilm developed on the surface of the anodic electrode.

Conflicts of interest

The authors disclose that they have no conflicting interests.

Acknowledgments

This study was funded financially supported by prof doctor Fatma Ibrahim El-Zamik, and the National Research Centre, Egypt. To her, I express my deepest gratitude for her keen supervision, suggested research point, tutorial guidance, and for her helpful advice, unlimited help, and continuous encouragement. We also are grateful to Prof. K.M. El-Khatib, Dr. Dena Z. Khater and Prof. Howaida M. L. Abd El-Basit for their support, valuable comments, honest supervision, sharing of their knowledge, continuous valuable instruction, beneficial advice, and for their time and effort in checking this study.

Table1: Performance comparison of MFC utilizing several ZnO-based electrocatalysts

Cathode catalyst	anode substance	Cathode substance	Substrate	MFC configuration	Microorganism	OCP (mV)	CCV (mV)	PD _{max} (mW.m ⁻²)	Ref.
ZnO/AC Zink oxide supported on activated carbon	Carbon felt	Carbon cloth	Sodium acetate	Air cathode	Activated sludge	562	300	90.177 (mW.m ⁻³)	This study
Polymer polyaniline PANI-Cu/ZnO	Stainless steel mesh	Stainless steel mesh	Wastewater	Double chamber	Wastewater from food waste	0.0902		45.12	[23]
CuO/ZnO Nanoparticles	Graphite plate	ZnO modified graphite plate	Milk AO7 (Acid Orang 7)	Double chamber	Anaerobic activated sludge	363.6		51.84	[24]
Go-Zn/Co Graphene oxid supported zinc and cobalt	Carbon cloth	Carbon cloth	Sodium acetate	Air cathode	Anaerobic digester sludge	880	145	773	[25]
CaFe _{0.7} Zn _{0.3} O ₃	Carbon felt	Carbon cloth	Sodium acetate	Double chamber	S. oneidensis	428		892.1 (mWm ⁻³)	[27]
rGO-CuS-ZnS reduced graphene oxide-copper sulfide-zinc sulfide	Carbon fiber brush	Carbon cloth	Sodium acetate	Air cathode		761		1692	[30]
Cel-PDA/ TiO:ZnO	Carbon cloth	Carbon cellophane cloth	Sodium acetate	Air cathode	Textile wastewater	1000	740	63	[31]
GO-ZnO/GO-TiO ₂	Self-fabricated	Graphite rod	Glucose	Double chamber	Cobalt upplemented wastewater	330	139	75.43	[39]
Co/Fe/N/CNT	Carbon paper	Carbon cloth	Glucose	Air cathode	E. coli K12	760	480	751	[40]
MnO ₂ /Pt	Carbon felt	Carbon felt	Palm oil	Air cathode	Anaerobic sludge	626		3.3	[41]
(Polymer-Ni-alumina: AC/CF	Carbon felt	Carbon felt	Artificial wastewater	Air cathode	E. coli	981		1270	[42]
Mn/AT/AC/GCE(A T:aminoantipyrine)	Carbon black	Graphite carbon	Artificial wastewater	Air cathode	Activated sludge	628		1600	[43]
Fe ₂ O ₃ coated anode and cathode	Carbon paper	Carbon paper	Sodium acetate	Double chamber	Activated sludge			30.81	[44]
Fe ₂ O/C Mn ₂ O ₃ /C	Carbon felt	Carbon fiber	Sodium acetate	Air cathode	Anaerobic mesophilic sludge	239.2 400.6		15Wm ⁻³ 32Wm ⁻³	[45]

References

- [1]. F. Davis and S.P. Higson, "Biofuel cells recent advances and applications," *Biosens Bioelectron.*, vol. 22, p. 1224, 2007.
- [2]. P. Choudhury, U. Shankar, P. Uday, T. K. Bandyopadhyay, R. N. Ray, and B. Bhunia, "Performance improvement of microbial fuel cell (MFC) using suitable electrode and Bioengineered organisms: A review," *Bioengineered*, vol. 8, no. 5, pp. 471–487, 2017.
- [3]. A. D. Kavya, S. J. Huang and C. T. Wang, "Integration of various technology-based approaches for enhancing the performance of microbial fuel cell technology: A review," *J. Chemosphere*, vol. 287, P. 3, 2022.
- [4]. G. Palanisamy, H.Y. Jung, T. Sadhasivam, M.D. Kurkuri, S.C. Kim, and S.H. Roh, "A comprehensive review on microbial fuel cell technologies: Processes, utilization, and advanced developments in electrodes and membranes," *J. Clean. Prod.*, vol. 221, pp.598–621, 2019.
- [5]. S. Sui, X. Wang, X. Zhou, Y. Su, S. Riffat, and C. Liu, "A comprehensive review of Pt electrocatalysts for the oxygen reduction reaction: nanostructure, activity, mechanism and carbon support in PEM fuel cells," *J. Mater. Chem. A.*, vol. 5, pp. 1808–1825, 2017.
- [6]. M. Shao, Q. Chang, J. P. Dodelet, and R. Chenitz, "Recent advances in electrocatalysts for oxygen reduction reaction," *Chem. Rev.*, vol. 116, pp. 3594–3657, 2016.
- [7]. R. Kumar, L. Singh, Z.A. Wahid, and M. Fadhil, "Exoelectrogens in microbial fuel cells towards bioelectricity generation: A review," *Int. J. Energy Res.*, vol. 39, p. 1048, 2015.
- [8]. A. Parkash, "Microbial Fuel Cells: A Source of Bioenergy," *J. Microb Biochem Technol.*, vol. 8, pp. 247–255, 2016.
- [9]. T. Cai, L. Meng, G. Chen, Y. Xi, N. Jiang, J. Song, S. Zheng, Y. Liu, G. Zhen, and M. Huang, "Application of advanced anodes in microbial fuel cells for power generation: A review," *Chemosphere*, vol. 248, p. 125985, 2020.
- [10]. S. Mateo, M. Mascia, Fernandez-Morales, F. J. Rodrigo, and M. A. Di Lorenzo, "Assessing the impact of design factors on the performance of two miniature microbial fuel cells," *Electrochim. Acta*, vol. 297, pp. 297–306, 2019.
- [11]. B.H. Kim, I.S. Chang, and G.M. Gadd, "Challenges in microbial fuel cell development and operation," *Appl. Microbiol. Biotechnol.*, vol. 76, p. 485, 2007.
- [12]. C. Santoro, A. Serov, L. Stariha, M. Kodali, J. Gordon, S. Babanova, O. Bretschger, K. Artyushkova and P. Atanassov, "Iron based catalysts from novel low-cost organic precursors for enhanced oxygen reduction reaction in neutral media microbial fuel cells," *Energy Environ Sci.*, vol. 9, pp. 2346–2353, 2016.
- [13]. J. Huang, N. Zhu, T. Yang, T. Zhang, P. Wu, and Z. Dang, "Nickel oxide and carbon nanotube composite (NiO/CNT) as a novel cathode non-precious metal catalyst in microbial fuel cells," *Biosens Bioelectron*, vol. 72, pp. 332–339, 2015.
- [14]. W.F. Chen, Y.X. Huang, D.B. Li, H.Q. Yu, and L.F. Yan, "Preparation of a macroporous flexible three dimensional graphene sponge using an ice-template as the anode material for microbial fuel cells," *RSC Adv.*, vol. 4, pp. 21619–21624, 2014.
- [15]. Y.R. He, X. Xiao, W.W. Li, G.P. Sheng, F.F. Yan, H.Q. Yu, H. Yuan, and L.J. Wu, "Enhanced electricity production from microbial fuel cells with plasma-modified carbon paper anode," *Phys. Chem. Chem. Phys.*, vol. 14, pp. 9966–9971, 2012.
- [16]. D. Z. Khater, R. S. Amin, M. O. Zhran, Z. K. Abd El-Aziz, M. Mahmoud, H. M. Hassan and K. M. El-Khatib, "The enhancement of microbial fuel cell performance by anodic bacterial community adaptation and cathodic mixed nickel–copper oxides on a grapheme electrocatalyst," *J. Genet. Eng. and Biotechnol.*, vol. 20, no. 1, pp.1–16, 2022.
- [17]. S.L. Chen, G.H. He, A.A. C. Martinez, S. Agarwal, A. Greiner, H.Q. Hou, and U. Schroder, "Electrospun carbon fiber mat with layered architecture for anode in microbial fuel cells," *Electrochem. Commun*, vol. 13, pp. 1026–1029, 2011.
- [18]. E. Taskan, and H. Hasar, "Comprehensive comparison of a new tin-coated copper mesh and a graphite plate electrode as an anode material in microbial fuel cell," *Appl. Biochem. Biotechnol.*, vol. 175, pp. 2300–2308, 2015.
- [19]. Z. Zhang, X. Song, Y. Chen, J. She, S. Deng, N. Xu, and J. Chen, "Controllable preparation of 1-D and dendritic ZnO nanowires and their large area field-emission properties," *J. Alloy. Compd.*, vol. 690, pp.304–314, 2017.
- [20]. S.J. Chang, B.G. Duan, C.H. Hsiao, C.W. Liu and S.J. Young, "UV enhanced emission performance of low temperature grown Ga-doped ZnO nanorods," *IEEE Photonics Technol. Lett.*, vol. 26, pp.66–69, 2014.
- [21]. M. Shehata, S. El-Shafey, N. A. Ammar, A. M El-Shamy, "Reduction of Cu⁺² and Ni⁺² ions

- from wastewater using mesoporous adsorbent: effect of treated wastewater on corrosion behavior of steel pipelines,” *Ejchem*, vol. 62, pp 1587-1602, 2019.
- [22]. I. Abdelfattah, W. Abdelwahab, A. El-Shamy, “Montmorillonitic clay as a cost effective, eco friendly and sustainable adsorbent for physicochemical treatment of contaminated water,” *Ejchem*, vol. 65, pp 687-694, 2022.
- [23]. S. Mathew and P. C. Thomas, “Fabrication of polyaniline nanocomposites as electrode material for power generation in microbial fuel cells,” *Materials Today: Proceedings*, vol. 33, pp 1415-1419, 2020.
- [24]. R. T. Khajeh, A. Soheil, and K. Nofouzi, “Efficient improvement of microbial fuel cell performance by the modification of graphite cathode via electrophoretic deposition of CuO/ ZnO,” *Materials Chemistry and Physics*, vol. 240, p. 122208, 2020.
- [25]. W. Yang, G. Chata, Y. Zhang, Y. Peng, J.E. Lu, N. Wang, R. Mercado, J. Li, and S. Chen, “Graphene oxide-supported zinc cobalt oxides as effective cathode catalysts for microbial fuel cell: High catalytic activity and inhibition of biofilm formation,” *Nano Energy*, vol. 57, pp. 811-819, 2019.
- [26]. J. Yu, T. Huang, Z. Jiang, M. Sun and C. Tang, “Synthesis and Characterizations of Zinc Oxide on Reduced Graphene Oxide for High Performance Electrocatalytic Reduction of Oxygen,” *Molecules*, vol. 23, no. 3227, pp. 1-10, 2018.
- [27]. Y. Dai, L. Han, Y. Wang, K. Zhong, H. Zhang, J. Yu, Z. Huang, J. Yan, L. Huang, X. Liu, Y. Lu, X. Tao and S. Minhua, “Zn-doped CaFeO₃ perovskite-derived high performed catalyst on oxygen reduction reaction in microbial fuel cells,” *J. Power Sources*, vol. 489, p. 229498, 2021.
- [28]. Y. Wang, G.-Q. Zhou, J. Guo, and T. Q. Liu, “Controllable preparation of porous ZnO microspheres with a nio some soft template and their photocatalytic properties,” *Ceram. Int.*, vol. 42, pp. 12467–12474, 2016.
- [29]. B.R. Camacho, C. Morais, M.A. Valenzuela, N. Alonso and V. Catal, “Enhancing oxygen reduction reaction activity and stability of platinum via oxide-carbon composites,” *Today*, vol. 202, pp.36-43, 2013.
- [30]. S. Mahalingam, S. Ayyaru, and Y. H. Ahn, “Facile one-pot microwave assisted synthesis of rGO-CuS-ZnS hybrid nanocomposite cathode catalysts for microbial fuel cell application,” *Chemosphere*, vol. 278, p. 130426, 2021.
- [31]. R.S. Bahamonde, B. D. Chinchin, D. Arboleda, Y. Zhao, P. Bonilla, B. V. Bruggen, and P. Luis, “Effect of the bio-inspired modification of low-cost membranes with TiO₂: ZnO as microbial fuel cell membranes,” *Chemosphere*, vol. 291, p. 132840, 2022.
- [32]. R. A. Mirzaie and F. Hamed, “Introducing Pt/ZnO as a new non carbon substrate electro catalyst for oxygen reduction reaction at low temperature acidic fuel cells,” *Iranian J. Catalysis*, vol. 5, no. 3, pp. 275-283, 2015.
- [33]. X. Gong, S. You, X. Wang, Y. Gan, R. Zhang, and N. Ren, “Silver-tungsten carbide nanohybrid for efficient electrocatalysis of oxygen reduction reaction in microbial fuel cell,” *J. Power Sources*, vol. 225, pp.330–337, 2013.
- [34]. S. Rojas-carbonell, C. Santoro, A. Serov, and P. Atanassov, “Transition metal-nitrogen-carbon catalysts for oxygen reduction reaction in neutral electrolyte,” *Electrochem Commun.*, vol. 75, pp.38–42, 2017.
- [35]. A. D. Eaton, L.S. Clesceri, E.W. Rice “Standard Methods for the Examination of Water and Wastewater,” *American Public Health Association, Washington, DC*, 21st edn, 2005.
- [36]. D.E. Andrew, L.S. Clescenri, and A.E. Breenberg, “Standard Method for the Examination of Water and Wastewater,” nineteenth ed., Washington, DC, USA, APHA, AWW, WEF, 1995.
- [37]. M. Sun, G. Sheng, Z. Mu, X. Liu, Y. Chen, H. Wang, and H. Yu, “Manipulating the hydrogen production from acetate in a microbial electrolysis cell-microbial fuel cell-coupled system,” *J. Power Sources*, vol. 191, pp. 338–343, 2009.
- [38]. F. Papiya, A. Nandy, S. Mondal and P. Paban, “Co/Al₂O₃-rGO nanocomposite as cathode electrocatalyst for superior oxygen reduction in microbial fuel cell applications: The effect of nanocomposite composition,” *Electrochim Acta.*, vol. 254, pp. 1–13, 2017.
- [39]. A. A. Yaqoob, M. Nasir, M. Ibrahim, A. S. Yaakop and M. Rafatullah, “Utilization of biomass-derived electrodes: a journey toward the high performance of microbial fuel cells,” *Applied Water Science*, vol. 12, pp. 99-119, 2022.
- [40]. L. Deng, M. Zhou, C. Liu, L. Liu, C. Liu, and S. Dong, “Development of high performance of Co/Fe/N/CNT nanocatalyst for oxygen reduction in microbial fuel cells,” *Talanta*, vol. 81, pp. 444-448, 2010.
- [41]. M.R. Khan, “Nanostructured Pt/MnO₂ catalysts and their performance for oxygen reduction reaction in air cathode microbial,”

- World Acad. Sci. Eng. Technol. Trans. Energy Power Eng.*, vol. 9, 2015.
- [42]. S. Singh, A. Modi, and N. Verma, "Enhanced power generation using a novel polymer-coated nanoparticles dispersed-carbon micro-nanofibers-based air cathode in a membrane-less single chamber microbial fuel cell," *Int. J. Hydrogen Energy*, vol. 41, pp. 1237–1247, 2016.
- [43]. M. Kodali, C. Santoro, A. Serov, S. Kabir, K. Artyushkova, I. Matanovic, and P. Atanassov, "Air breathing cathodes for microbial fuel cell using Mn-, Fe-, Co and Ni-containing platinum group metal-free catalysts," *Electrochim. Acta*, vol. 231, pp. 115–124, 2017.
- [44]. A. Nandy, M. Sharma, S. V. Venkatesan, N. Taylo, L. Giegand, and V. Thangadurai, "Comparative Evaluation of Coated and Non-Coated Carbon Electrodes in a Microbial Fuel Cell for Treatment of Municipal Sludge," *Energies*, vol. 12, p. 1034, 2019.
- [45]. E. Martin, B. Tartakovsky, and O. Savadogo, "Cathode materials evaluation in microbial fuel cells: a comparison of carbon, Mn_2O_3 , Fe_2O_3 and platinum materials," *Electrochim. Acta*, vol. 58, pp. 58–66, 2011.